Advanced Testing and Characterization of Bituminous Materials –
Loizos, Partl, Scarpas & Al-Qadi (eds)
© 2009 Taylor & Francis Group, London, ISBN 978-0-415-55854-9

Size effect investigation on fracturing of asphalt concrete using the cohesive softening Discrete Element Model

H. Kim & M.N. Partl
Empa, Swiss Federal Laboratories for Materials Testing and Research, Dübendorf, Switzerland

M.P. Wagoner & W.G. Buttlar
University of Illinois at Urbana-Champaign, Illinois, USA

ABSTRACT: Cracking in asphalt concrete is one of the major causes of structural and functional deterioration of the pavement systems, particularly in cold climates. A clustered Discrete Element Method (DEM) was applied into the investigation of size effect on fracturing of asphalt concrete based on a disk-shaped compact tension (DC(T)) test. A bilinear cohesive softening model was implemented into the DEM framework to enable simulation of crack initiation and propagation in asphalt concrete. The influence of specimen size was investigated on the fracture of asphalt concrete using the homogeneous and heterogeneous DEM fracture models. The laboratory tests were conducted for specimen sizes of asphalt concrete varying from 100 mm to 450 mm in diameter. The DEM simulations were shown to compare favorably with experimental results and Bazant's size-effect law.

1 INTRODUCTION

The fracturing of asphalt concrete is a significant cause of premature pavement deterioration. Cracks at the pavement surface create a permanent maintenance liability, and those, which extend through the thickness of pavement, reduce structural capacity and greatly increase pavement permeability and the intrusion of moisture into the pavement foundation. There have been various efforts to investigate the fracture mechanism of asphalt concrete during the past several decades (Majidzadeh et al. 1971, Jacob et al. 1991, Jenq & Perng 1991). However, those fracture tests and numerical investigations were limited to a specific size range of the test specimen. Although the experimental and numerical results provided new insights towards the toughening mechanisms in the fracture of asphalt concrete, another area of interest is the influence of specimen size on the fracture behavior. This paper shows how the experimental fracture test and DEM fracture model are used to capture the dependency of specimen size. In the classical theories based on plasticity or limit analysis, the strength of geometrically similar structures are independent of the structure size. As already known, however, concrete structures and, in general, structures made of brittle or quasi-brittle materials do not follow this trend. The size effect is rigorously defined through a comparison of geometrically similar structures of different sizes. Based on the energy approach, Bazant (1984) developed a size-effect model that allows scaling for fracture energy. For example, a laboratory-sized specimen can be tested but large-scale fracture energy can be determined. Bazant used the phenomenon that, at very small sizes, a material will behave in a yield criterion, which is determined from classical mechanics. At the larger sizes, or if the material was brittle, linear elastic fracture mechanics (LEFM) is applicable. However, between these two sizes, the material behaves in a manner that lies somewhere between these two theories.

By testing different specimen sizes, but geometrically similar specimens, the fracture dependency of quasi-brittle material can be determined using the size-effect law. The equation that defines the size-effect law is:

$$\sigma_n = \frac{Bf_t}{\sqrt{1+\beta}} \tag{1}$$

where, σ_n is the nominal strength; f_t is the tensile strength; β is the brittleness number and is equal to d/d_0; d is the depth of the beam; and B and d_0 are empirical constants.

However, the influence of specimen size on fracture energy can be an issue in viscoelastic materials such as asphalt mixtures, polymers, etc. From the literature for Portland cement concrete (PCC) and test results from asphalt concrete (AC), properties such as tensile strength and fracture energy are specimen size dependent and require a scaling model in order to obtain a size-independent fracture property from laboratory tests.

2 EXPERIMENTAL TESTING

2.1 *Materials*

A Superpave® 9.5 mm NMAS mixture with a PG64-22 asphalt binder was used for DC(T) tests (Wagoner et al. 2005). The target gradation of mixture is shown in Table 1. The mixture was produced with a blend of three aggregate stockpiles, two of crushed dolomite limestone and one of natural sand. For asphalt mixtures compacted, asphalt binder contents were 5.25% and the targeted residual air void contents were 6.5%. The Superpave® indirect tension test (IDT) was used to determine the viscoelastic properties of the mixture and the indirect tensile strength (AASHTO T322-03 2004). The IDT test provided the creep compliance of the material at three temperatures (–20, –10, and 0°C). Time-temperature superposition principle was utilized to shift the creep data at the different temperature to a reference temperature to develop a master creep compliance curve. Figure 1. shows the master creep compliance curve for this material. The average indirect tensile strength of the mixture, measured at –10°C was 2.37 MPa.

Table 1. Material gradation curves.

Sieve size (mm)	12.5	9.5	4.75	2.36	1.18	0.6	0.3	0.15	0.075
Percentage by mass	100	99	77	49	24	15	10	7	6

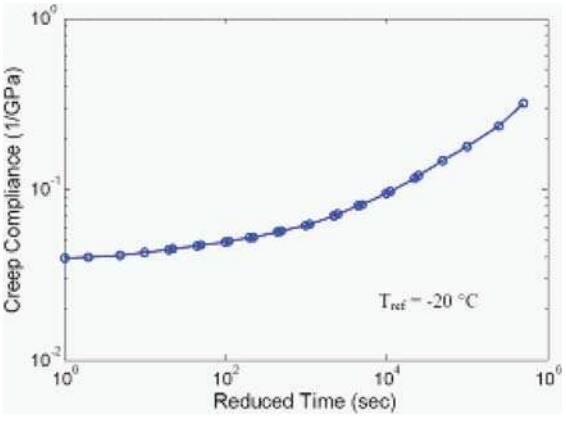

Figure 1. Master creep compliance curve for asphalt concrete.

2.2 *Fracture test*

A disk-shaped compact tension (DC(T)) specimen geometry was developed to investigate the fracture behavior of asphalt concrete and it has the ability to test cylindrical cores obtained from in-place asphalt concrete pavements and gyratory-compacted specimens fabricated during the asphalt concrete mixture design process for relevant fracture properties (Kim et al. 2008). Figure 2(a) shows the DC(T) test configuration inside a temperature chamber and a typical fractured specimen. The DC(T) test is loaded in tension through the loading holes and is conducted with a constant crack mouth opening displacement (CMOD) rate. The CMOD can be measured at the edge of the notched crack by a clip gauge. The standard specimen diameter is 150 mm and both cored hole diameters within the specimen are 25 mm. The width of the specimen (W) was 110 mm with the notch length (a) being 27.5 mm (a/W = 0.25). Therefore, the initial ligament length (W–a) was 82.5 mm. The thickness (t) of the specimen was 50 mm.

As shown in Figure 2(b), the limited size range of DC(T) fracture specimens were cored from the test pad built using standard asphalt paving equipment and procedures. DC(T) specimen with 450 mm diameter was not showed in Figure 2(b) although it was experimentally tested. A limitation was the current testing equipment used for fracture testing of asphalt concrete. Specifically, the temperature controlled environmental chamber would limit the maximum dimension to approximately 560 mm. The temperature chamber is crucial for testing asphalt concrete since the fracture properties are temperature dependent. Another limitation to specimen size was the ability to handle the specimen without incurring damage. For very large specimens, the self-weight of the specimen could induce deformations due to creep and introduce damage in the specimen. Therefore, the above limitations were taken into consideration to select the DC(T) geometry. The DC(T) specimen dimensions with varying diameters can be found in Table 2. Each specimen has the same thickness, 50 mm, to focus on the diametric size effects (i.e., ligament length). However, the thickness effect on fracturing of asphalt concrete should not be ignored and the scope is beyond this diametric size effect study.

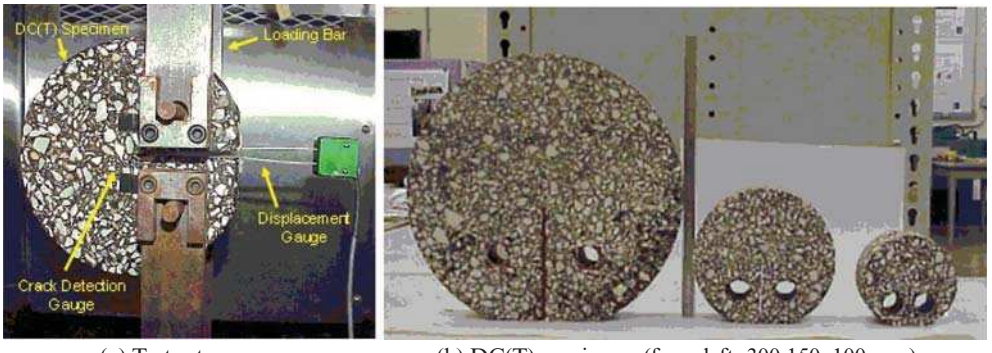

(a) Test set-up (b) DC(T) specimens (from left: 300,150, 100 mm)

Figure 2. DC(T) test setup and a typical fractured specimen.

Table 2. DC(T) specimen dimension for size effect analysis.

DC(T) Dimension (mm)				
D	100	150	300	450
W	73.3	110	216.3	330
a	18.3	27.5	54.1	82.5
d	16.7	25	49.2	75
C	23.3	35	68.8	105
Φ	35	35	35	35
t	50	50	50	50

The testing for all specimens was conducted at −10°C. The main purpose for using this temperature was to reduce the viscous response of the materials. The loading rate of the different sized specimens must be considered to ensure that the fracture energy comparison between the different sizes is valid. The reason for considering the loading rate is that fracture energy is dependent on the rate of loading. The crack mouth opening displacement (CMOD) was used as the measurement for closing the servo-hydraulic control loop. The standard CMOD rate for the DC(T) was 1 mm/min for the standard geometry. The loading rates for other specimen sizes are 0.667 mm/min for 100 mm, 2 mm/min for 300 mm, and 3 mm/min for 450 mm diameter specimen, respectively to make the CMOD rate constant.

3 NUMERICAL MODELING

3.1 *Constitutive law*

The discrete element method (DEM) originally developed by Cundall (1971) has proven to be a powerful and versatile numerical tool for modeling the behavior of granular and particulate systems, and also for studying the micromechanics of materials such as soil at the particle level. The DEM discretizes a material using rigid elements of simple shape that interact with neighboring elements according to interaction laws that are applied at points of contact. In this paper, discrete element modeling (DEM) is performed using the commercial software package, PFC-2D, which utilizes fixed-size and fixed-shape circular elements that can be used to approximate bulk material stress-strain behavior (ITASCA 2002).

The translational and rotational stiffnesses ([*K*]) of a particle relate increments of force and moment (Δf) to increments of displacement (δu) and rotation via the matrix relations:

$$\{\Delta f\} = [K]\{\delta u\} \tag{2}$$

The linear contact stiffness (K^n or K^s) is defined by the normal and shear particle stiffness k_n and k_s (force/displacement) of the two contacting entities (ball-to-ball or ball-to-wall) acting in series. Based on the strain energy density and Hooke's law, the relationship between the discrete element springs and the elastic properties of a plane strain conditions are given by (Morikawa et al. 1993).

$$K^n = \frac{E}{\sqrt{3}(1+\nu)(1-2\nu)} \tag{3}$$

$$K^s = \frac{E(1-4\nu)}{\sqrt{3}(1+\nu)(1-2\nu)} \tag{4}$$

Cohesive zone models (CZMs) have recently been used to simulate the fracture process in a number of material systems under a variety of loading conditions. In the fracture study of asphalt concrete discussed herein, the bilinear cohesive fracture model, as shown in Figure 3,

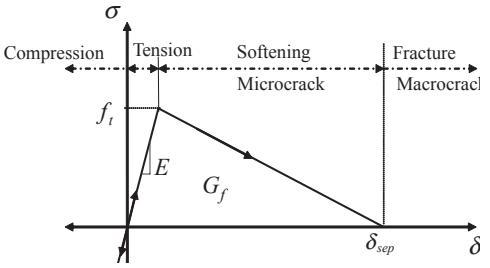

Figure 3. Cohesive fracture model.

was selected due to the effectiveness of assigning fracture parameters such as tensile strength (f_t) and fracture energy (G_f). The shape function of cohesive fracture model can be varied and it depends on the material behavior.

3.2 *DEM mesh*

By integrating of numerical simulation with size effect experiments, a better understanding of the fracture process in asphalt concrete and its relation to specimen size was obtained. Figure 4 shows the detail description of homogeneous fracture model with bulk viscoelastic contacts. The mechanical loadings with constant velocities were applied to numerical loading bars inside of specimen holes like in laboratory tests. The cohesive fracture contacts, which were represented by solid lines between particles, were inserted into the middle of specimen ligament and the viscoelastic contacts were assigned into the whole specimen area. The radius of circular elements used to approximate the material fracture behavior was 0.5 mm, which was smaller than the notched crack width, 2 mm. However, the "real" crack tip width can be smaller than the element size used here. The notched crack length was from 41.6 mm to 187.5 mm depending on the different specimen sizes.

Also, the details of heterogeneous DEM mesh can be found in Figure 2(b). Each aggregate is composed of various numbers of particle meshes, which depend on the aggregate size and shape. Based on an image processing procedure, the two-dimensional microstructure of asphalt specimen can be obtained and projected into DEM mesh. More details of image processing technique can be found in author's previous publication (Kim et al. 2008).

3.3 *Material parameters*

The fracture parameters, i.e., 3.56 MPa for tensile strength and 344 N/m for fracture energy, were determined by the indirect tensile test (IDT) and DC(T) fracture test at –10°C. Also, the viscoelastic properties were obtained from creep tests conducted at multiple temperatures, and shift factors are evaluated from shifting the compliance versus time curve at different temperatures in a log scale to establish a smooth and continuous curve. Interconversion of the time dependent creep compliance function yields a relaxation modulus given as

$$E(\xi) = \sum_{i=1}^{N+1} E_i (1 - e^{-\xi/\tau_i}) \tag{5}$$

where, $E(\xi)$ is a relaxation modulus at the reduced time of ξ, and E_i and τ_i are model constants for the master relaxation modulus curve.

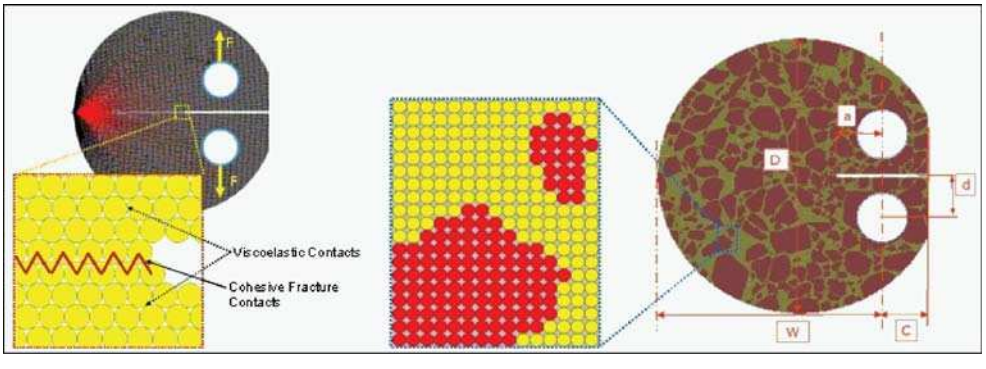

(a) Homogeneous model mesh (b) Heterogeneous model mesh

Figure 4. Description of homogeneous fracture model.

Table 3. Burger's model parameters.

Maxwell		
Stiffness (N/m)	Viscosity (Ns/m)	Poisson's ratio
9.260E+8	1.601E+12	0.25
Kelvin		
Stiffness (N/m)	Viscosity (Ns/m)	Poisson's ratio
4.995E+8	4.998E+10	0.25

For the viscoelastic simulation, Burger's model was inserted at each particle contact point. The determined relaxation modulus can be converted to the DEM contact stiffness based on Equation (3), Equation (4), and Equation (5) as shown in Table 3.

4 RESULTS AND COMPARISIONS

4.1 *Homogeneous fracture results*

Figure 5 presents the comparisons of global responses between experimental and numerical results for three different specimen sizes (100 mm, 150 mm, and 300 mm). Elastic and viscoelastic models were compared using force versus CMOD curves to investigate both elastic and viscoelastic model capabilities in the fracture prediction of asphalt concrete. The same fracture parameters were selected for fracture simulations with different specimen sizes. Same loading rates as in experimental tests were applied in the numerical simulations. The results show that the elastic simulations deviate far from the experimental results as the DC(T) specimen size increases. Larger specimen has greater amount of viscoelastic dissipated strain energy. Therefore, the effect of viscoelastic behavior is getting significant in the larger specimens.

Using Bazant's size effect law, the nominal strength versus the characteristic dimension was illustrated as shown in Figure 6. The nominal strength was calculated by dividing the peak load P with the ligament area. The characteristic dimension was selected as the depth, W, of the specimens. The depth was selected for determining the geometric factors required to determine the specific fracture energy (G_f). The size dependency of asphalt concrete on the nominal strength has a similar trend to that of Portland cement concrete. The results for the homogeneous DEM fracture model with bulk viscoelastic properties were found to agree with experimental results. For the homogeneous viscoelastic DEM model, the same material parameters for each set were used in the fracture simulations for all different specimen sizes to verify if DEM models can capture the specimen size dependency or not.

4.2 *Heterogeneous fracture results*

Using the high-resolution image technique, the coordination of microstructure in asphalt specimens was successfully obtained and projected into the DEM mesh to investigate various heterogeneous fracture behaviors. The bulk and fracture parameters were determined from modulus, strength, and fracture tests for each material (i.e., aggregate, mastic) and the interface parameters could be determined based on the known parameters and inverse analysis [Kim 2007]. The determined input parameters are shown in Table 4. As shown in Figure 7, DC(T) DEM specimens which capture the sand-size and larger aggregate features of 9.5 mm nominal maximum aggregate size (NMAS) mixtures could be obtained.

Although the homogeneous viscoelastic DEM fracture model can predict specimen size effect in quasi-brittle materials, it was desired to study size effect using a heterogeneous DEM fracture model. However, it was difficult to handle the microstructure of large size specimen using the image techniques employed in this study due to the limitation of image resolution

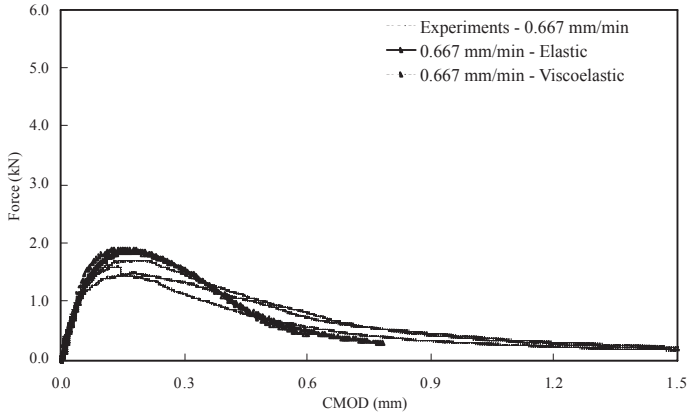

(a) 100 mm

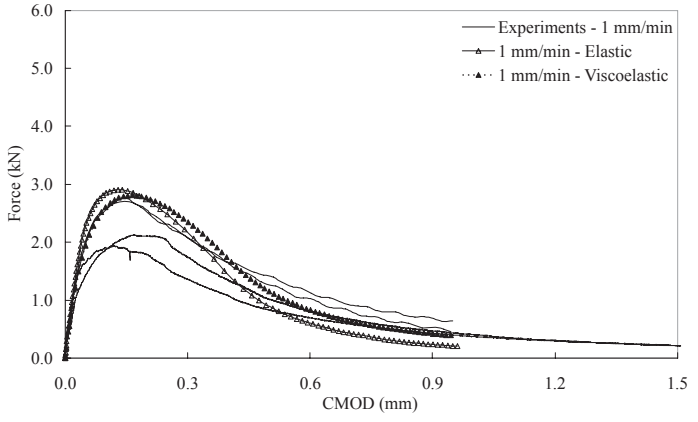

(b) 150 mm

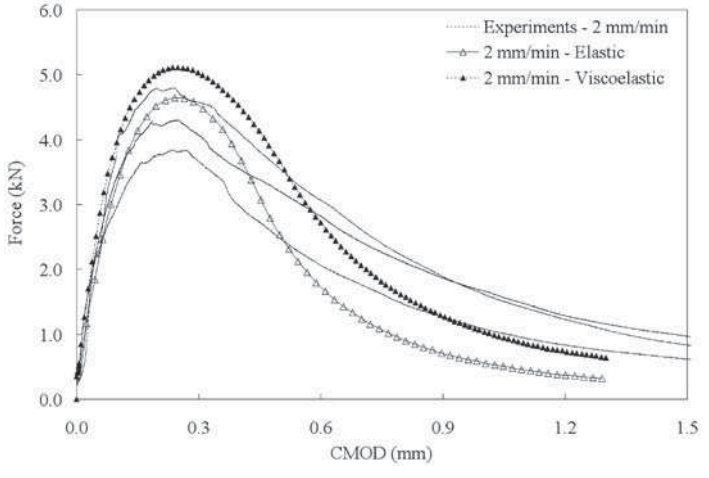

(c) 300 mm

Figure 5. Comparisons between homogeneous DC(T) fracture models and experimental tests.

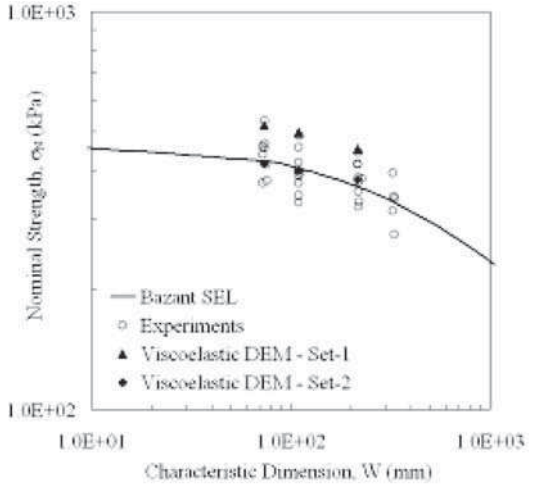

Figure 6. Nominal strength versus specimen size.

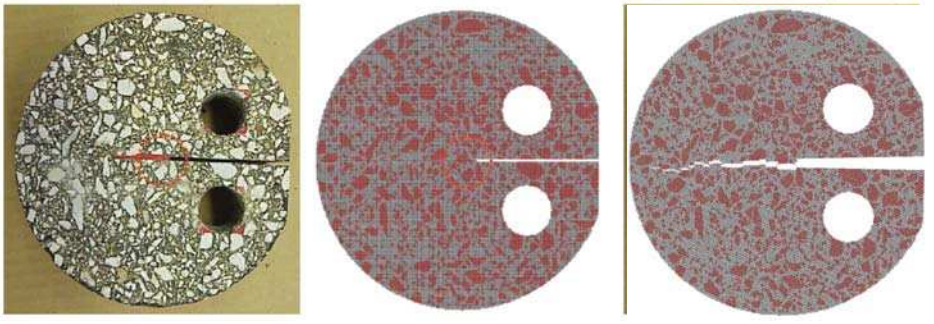

(a) Experimental specimen image (b) DEM specimen (c) Failed DEM specimen

Figure 7. Heterogeneous DEM model mesh and multi-phase material properties.

Table 4. Material parameters for heterogeneous DEM fracture model.

DC(T) at –10°C with PG64-22			Material properties	
Specimen size (mm)	Phase	Poisson's ratio	Young's modulus (GPa)	Tensile strength (MPa)
100, 150, 300	Aggregate	0.15	56.8	6.59
	Mastic	0.25	11.4	2.87
	Interface	0.25	11.4	2.61

and the large image size, which is computationally intensive to process. Figure 9 shows the global responses of heterogeneous fracture models compared with experimental results from 100 mm to 300 mm specimens. The heterogeneous fracture model has material properties calibrated based on the fracture energies obtained from experimental tests for different specimen sizes. The global response of heterogeneous fracture model with 100 mm diameter was slightly over-predicted as shown in Figure 9(a). Due to the small difference in the ligament length between 100 mm and 150 mm specimen, the response difference was not significant.

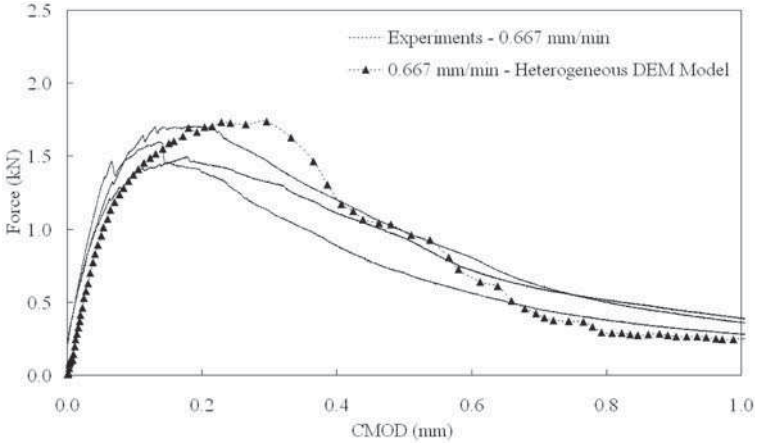

(a) D = 100 mm

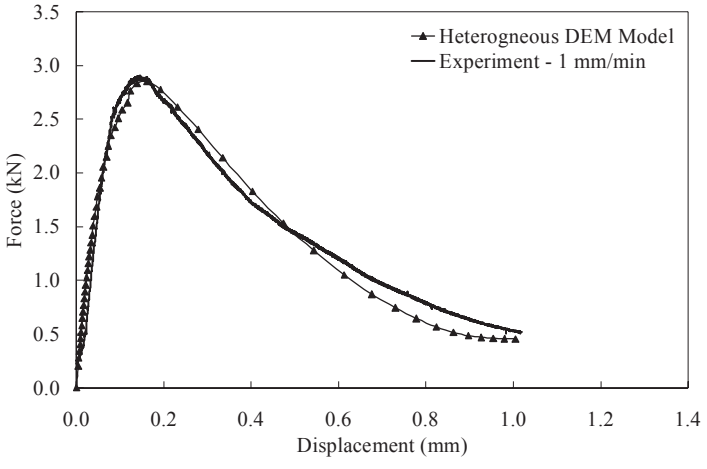

(b) D = 150 mm

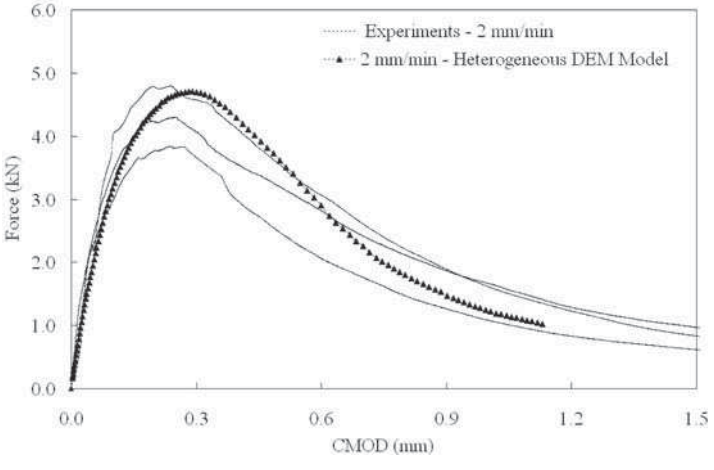

(c) D = 300 mm

Figure 9. Comparisons between heterogeneous DC(T) fracture models and experimental tests.

5 CONCLUSIONS

A micromechanical fracture modeling approach has been employed to investigate the specimen size effect and toughening mechanism in the fracture of asphalt concrete. Cohesive softening model was employed to analyze asphalt fracture behaviors based on the discrete element method. DC(T) fracture tests were conducted for different sizes of asphalt concrete varying from 100 mm to 450 mm diameter but the 450 mm specimen was not simulated with the DEM fracture model due to the limitation of the high computational time and the handling difficulty of specimen image. The fracture energies determined by experiments were varied for the different specimen sizes. Different size specimens were modeled and simulated using homogeneous DEM fracture models with bulk viscoelastic properties. The experimental and numerical specimen size dependency of asphalt concrete was compared with the size effect law, which was proposed by Bazant.

The bulk viscoelastic DEM fracture model with the same material properties could predict the size effect on the nominal strength of asphalt concrete based on two sets of material properties. By comparing with elastic and viscoelastic homogeneous DEM fracture models, it was shown that viscoelastic properties of asphalt concrete play an important role on the fracture behavior as the specimen size becomes larger. The heterogeneous fracture model for different specimen size could be implemented and applied for the investigation of size effects but the calibration procedure of material parameters is necessary based on experimental test data. The global fracture responses of heterogeneous DEM models were matched well with experimental fracture behaviors in the force versus CMOD curves. For the large size of DEM, the fast contact algorithm or simplified approach is much needed to investigate the fracture behavior of asphalt concrete. 3-D fracture analysis should be conducted to investigate more realistic fracture behavior and the specimen thickness effect on the fracture of asphalt concrete. However, the computational running time should be considered for both large size and three-dimensional fracture analyses and will be limited in size of the numerical simulation by current.

REFERENCES

AASHTO T322-03. 2004. Standard test method for determining the creep compliance and strength of hot mix asphalt (HMA) using the indirect tensile test device. *Standard Specifications for Transportation Materials and Methods of Sampling and Testing*, 24th Edition.

Bazant, Z.P. 1984. Size effect in blunt fracture: concrete, rock, metal. *ASCE Journal of Engineering Mechanics* 110: 518–535.

Cundall, P.A. 1971. A computer model for simulating progressive, large-scale movements in blocky rock systems. *Proceedings of the International Symposium of Rock Fracture*, Nancy, France.

ITASCA Inc. 2002. *PFC 2D Version 3.0*. Minneapolis, Minnesota 55415, USA.

Jacob, M.M., Hopman, P.C. and Molenaar, A.A.A. 1991. Application of fracture mechanics in principles to analyze cracking in asphalt concrete. *Journal of Asphalt Paving Technologists* 65: 1–39.

Jenq, Y. and Perng, J. 1991. Analysis of crack propagation in asphalt concrete using cohesive crack model. *Transportation Research Record* 1317: 90–99.

Kim, H. 2007. *Investigation of toughening mechanisms in the fracture of asphalt concrete using the clustered discrete element method*. Ph.D. Thesis, University of Illinois at Urbana-Champaign.

Kim, H., Wagoner, M.P. and Buttlar, W.G. 2008. Simulation of heterogeneous cohesive fracture model in asphalt concrete using discrete element method. *ASCE Journal of Materials in Civil Engineering* 20(8): 552–563.

Majidzadeh, K., Kauffmann, E.M. and Ramsamooj, D.V. 1971. Application of fracture mechanics in the analysis of pavement fatigue. *Journal of Asphalt Paving Technologists* 40: 227–246.

Morikawa, H., Sawamota, Y. and Kobayashi, N. 1993 Local fracture analysis of a reinforced concrete slab by the discrete element method. *Proceedings of the Second International Discrete Element Methods*, MIT Press, Cambridge, MA, USA.

Wagoner, M.P., Buttlar, W.G. and Paulino, G.H. 2005. Disk-shaped compact tension test for asphalt concrete fracture. *Experimental Mechanics* 45(3): 270–277.